Effect of the mode composition disturbances in a high-enthalpy wind tunnel on wave processes in the hypersonic viscous shock layer

S V Kirilovskiy[1,2], T V Poplavskaya[1,2] and I S Tsyryulnikov[1,2]

[1]Khristianovich Institute of Theoretical and Applied Mechanics SB RAS, 630090 Novosibirsk, Russia
[2]Novosibirsk State University, 630090, Novosibirsk, Russia

Email: kirilov@itam.nsc.ru, popla@itam.nsc.ru

Abstract. A numerical and experimental study of the spectral distribution of disturbances hot-shot wind tunnel was performed. It was found that disturbances are the superposition of fast acoustic waves propagating along axial direction and oblique slow acoustic waves which have less amplitude. Numerical simulation of disturbances evolution in the nozzle of the wind tunnel was carried out by solving 2D Navier–Stokes equations using the ANSYS Fluent program package. Experiments were carried out in the IT-302M high-enthalpy hotshot wind tunnel ITAM SB RAS.

1. Introduction

Characteristics of the incoming flow disturbances, in particular the mode composition, is important for the objectives of the study of receptivity and disturbances evolution in supersonic and hypersonic shock layers. A viscous shock layer is always formed on the leading edges of hypersonic aircraft. The peculiarity of hypersonic shock layer is a closeness of boundary layer to the bow shock and considerable thickness of boundary layer. Disturbances generated in the shock layer propagate downstream and affect the laminar-turbulent transition in a hypersonic boundary layer of the whole aircraft (figure 1). Khristianovich Institute of Theoretical and Applied Mechanics SB RAS has considerable experience in experimental and numerical simulation of hypersonic instability in the viscous shock layer on the plate at the Mach numbers from 10 up to 21 [1-4].

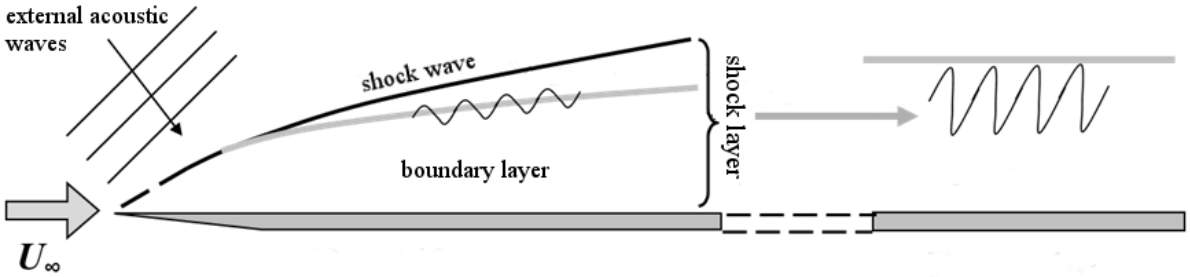

Figure 1. Viscous shock layer and evolution of the freestream flow disturbances

The transition in the compressible boundary layers has been the subject of research for many years, but only a limited number of existing experimental and numerical investigations have been conducted for the high-enthalpy hypersonic flows. Flight studies of gas flow stability are constructively complex and quite expensive. For this reason, numerical simulation and wind tunnel experiments are important. Experimental data on receptivity and evolution of disturbances in wind tunnels are widely used for constructing reliable theoretical models of the laminar-turbulent transition. However, it is difficult to estimate characteristics of disturbances without taking into account the processes in the nozzle channel of wind tunnel where the flow is formed. Therefore the free-stream processes (proceeding in the wind tunnel nozzle) have to be included in disturbance evolution simulations.

Thus the problem of disturbances evolution in hypersonic flow over plate is solved in three stages. In the beginning, the numerical simulation of flow in the nozzle of wind tunnel (figure 2) was performed and the flow parameters on the nozzle outlet were obtained. Then using the obtained data, the problem of flow over the plate in the test section of the wind tunnel was solved. Third stage was solving the transient problem of interaction between viscous shock layer and freestream plane acoustic waves. The knowledge of the mode composition of disturbances in the flow, i.e., separation of the field of disturbances of a supersonic flow into vortex, entropy, and acoustic modes, is important for refining the results of the problem of the perturbations evolution.

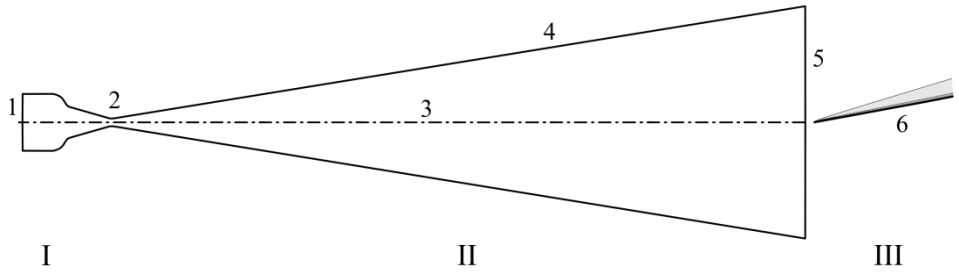

Figure 2. Sketch of the nozzle channel IT-302 M ITAM SB RAS: I – prechamber, II –conic nozzle, III – test chamber, 1 – inlet section, 2 – critical section, 3 – axis of symmetry, 4 – nozzle wall, 5 – output section, 6 – plate

The problem of determining the mode composition of disturbances in the nozzle channel of hotshot wind tunnel IT- 302M ITAM SB RAS is solved in this paper by using the numerical-experimental method.

2. Experiments in the wind tunnel

Experiments were carried out in the IT-302M high-enthalpy hotshot wind tunnel (Khristianovich Institute of Theoretical and Applied Mechanics, Siberian Branch, Russian Academy of Sciences) under conditions of air efflux from the nozzle at the following flow parameters: $M_\infty = 5.7$; $Re_{1\infty} = 8\times10^6$ m^{-1}. The gas was heated by an electric discharge in the prechamber of the wind tunnel. A high-speed digital camera (Phantom 310) operating at a frame rate of 120 kHz was used to obtain a sequence of the schlieren images of visualized flow in the test chamber. Then a sequence of frames was processed by the algorithm described below to determine the longitudinal phase velocity of the perturbation.

Figure 3 shows a plot of longitudinal phase velocity U_f of pressure disturbance propagation versus frequency, where the upper dashed straight line 1 corresponds to phase velocity $U_f = U_\infty + c_\infty$ of the fast acoustic mode, solid line 2 corresponds to phase velocity $U_f = U_\infty$ of the entropy and vortex modes, and lower dash–dot line 3 corresponds to phase velocity $U_f = U_\infty - c_\infty$ of the slow acoustic mode (where c_∞ is the velocity of sound in the incoming flow). As can be seen, the experimental points are placed close to the upper line, which indicates that the longitudinal phase velocity of pressure disturbances in the IT-302M wind tunnel corresponds to the phase velocity of fast acoustic waves.

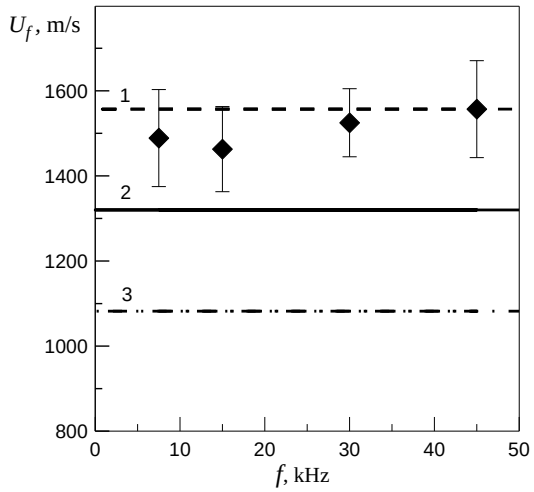

Figure 3. Frequency dependences of the longitudinal phase velocity U_f of pressure disturbances in the IT-302M wind tunnel (airflow, $M_\infty = 5.7$; $Re_{1\infty} = 8\times10^6$ m^{-1}): 1 – fast acoustic mode, 2 –entropy-vortex mode, and 3 – slow acoustic mode; points – experimental data [3]

3. Numerical simulations

Numerical simulation of disturbances evolution in the nozzle of the wind tunnel IT-302M was carried out by solving 2D Navier–Stokes equations in axisymmetric formulation with k-ω SST turbulence model using the ANSYS Fluent program package with a density-based solver applied to an implicit second-order accuracy (in space) scheme with Roe-FDS convective flow splitting and explicit 4-stage Runge–Kutta scheme in time. The thermal conductivity and viscosity of a working gas were set by a formula from the kinetic theory and by Sutherland's law, respectively, and the heat capacity was taken to be a function of temperature.

Computational domain was constructed geometrically similar to the real channel of the wind tunnel IT-302M (see figure 2). It was covered by a rectangular grid with clustering near the critical section and nozzle walls (a total of 600000 meshes). The values of total temperature and total pressure T_0=3000K, P_0=200bar in the prechamber of the wind tunnel were set at the left boundary of the computational domain (beginning of the nozzle channel). The solution on the right boundary (end of the nozzle channel) was extrapolated from inside the computational domain. Non-slip conditions and the constant wall temperature T_w = 300 K were set at the nozzle wall, and the symmetry condition was set at the lower boundary (the nozzle axis).

Disturbances in the prechamber appear due to the impact of electric discharge gas. In numerical simulations of these disturbances, the variables on the left boundary of the computational domain were set as a superposition of the steady stagnation parameters and a plane monochromatic acoustic wave in the form (with using user defined functions embedded in the computational code):

$$P_0^* = P_0 + \acute{P}_0 \cdot sin(-2\pi f_0 \cdot t)$$

$$T_0^* = T_0 + \frac{(\gamma-1)}{\gamma}\frac{\acute{P}_0 \cdot \bar{T}_0}{\bar{P}_0} sin(-2\pi f_0 \cdot t)$$

P_0, T_0–total pressure and total temperature, $\acute{P}_0$–amplitude of total pressure disturbances, f_0 –frequency of disturbances. The total amplitude of the pressure pulsations set equal to $\acute{P}_0 = 0.03P_0$, in the present calculations and pulsation frequency f_0 = 40kHz.

Figure 4 shows instantaneous field of pressure fluctuations, normalized on local pressure values. It is seen that disturbances propagate both along the nozzle axis and turbulent boundary layer on the nozzle wall.

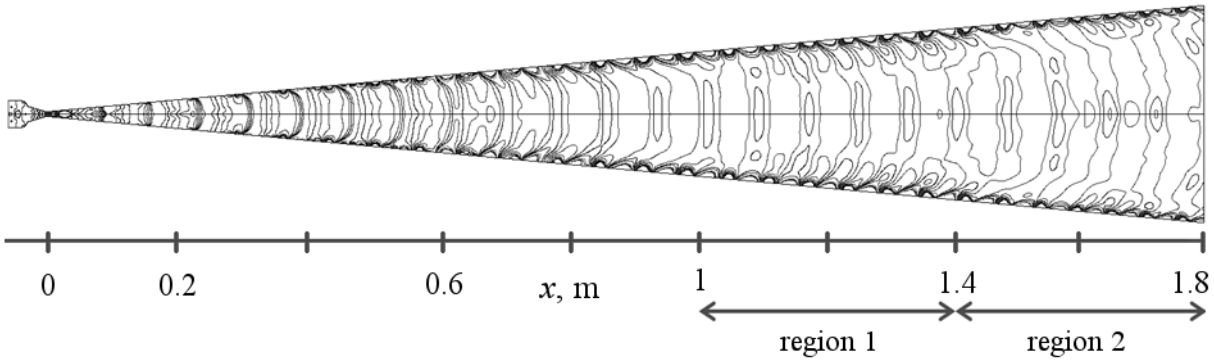

Figure 4. Instantaneous field of pressure fluctuations in the nozzle channel, normalized on local pressure values: $\acute{P}_0 = 0.03 \cdot P_0$, f_0 =40kHz

4. Algorithm of longitudinal wave numbers determination

Determination of longitudinal wave numbers of disturbances k_x was performed using following algorithm shown in figure 5. Time series of static pressure values p(x,t) along x axis from the range 1-1.8m were processed by using the Fourier transform to obtain amplitude spectra $A_f(x,f)$ in each point along x axis from this range.

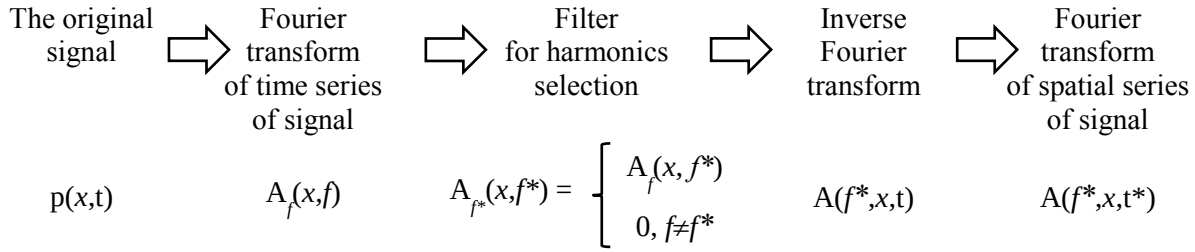

Figure 5. Algorithm of determination of longitudinal wave numbers of disturbances

Amplitude spectra of averaged pressure fluctuations over whole considered x range are shown in figure 6. It is seen that disturbances propagate both with main frequency f_0=40kHz and harmonic frequency f_1=80kHz in the nozzle channel.

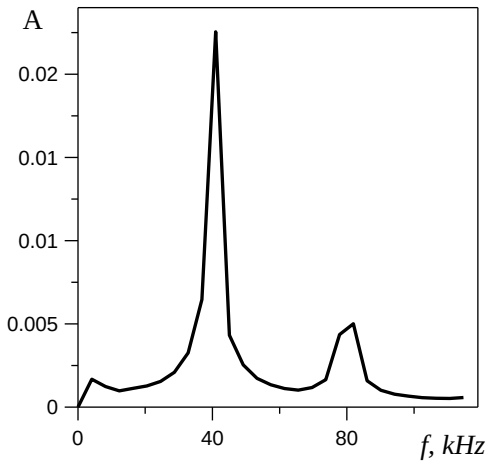

Figure 6. Amplitude spectra of pressure fluctuations averaged over whole considered x range

Then the filter was used to highlight the selected frequency f^*. The inverse Fourier transform is carried out after filtration procedures. This makes it possible to obtain the amplitude distribution $A(f^*,x,t)$ along the axis for a single harmonic f^*. After this the expansion of the data on a longitudinal wave numbers k_x was carried out at arbitrary time moment t*. This makes it possible to identify the disturbances modes.

Similarly schlieren imaging sequence of frames was used in the processing of experimental data and the signal of brightness from the time was processed.

5. Results and discussion

Figure 7 shows the dependence of the pressure pulsation amplitude from the longitudinal wave number for both frequencies $f^*=f_0$=40 kHz (figure 7a) and 80 kHz (figure 7b) and for two regions of the nozzle axis.

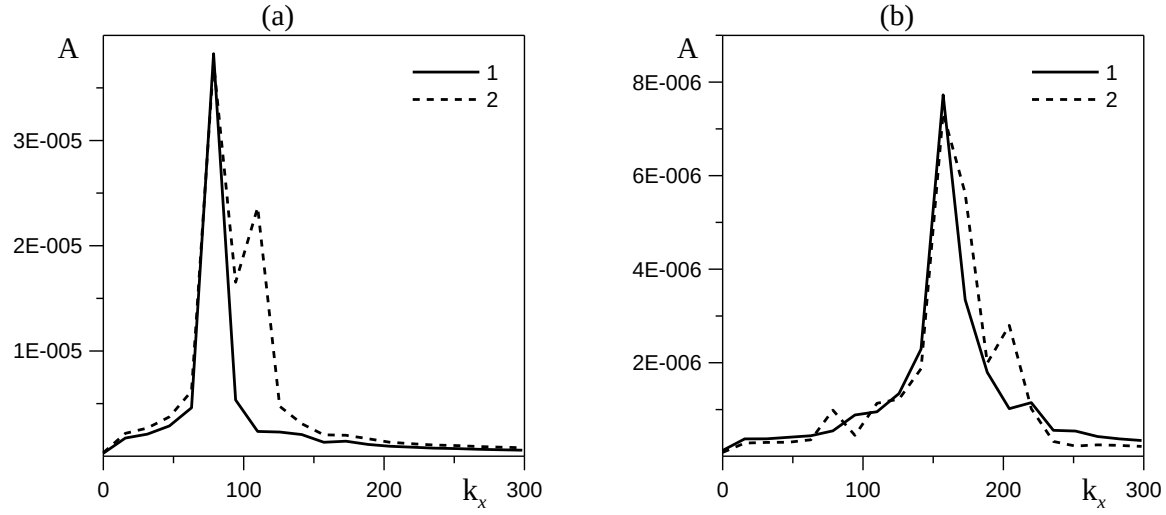

Figure 7. The spectral decomposition of the normalized amplitudes of the pressure pulsations at two regions along the axis of the nozzle on the longitudinal components of the wave vector: a – f_0 = 40 kHz, b – f_1 = 80 kHz, 1 – region corresponds to x from 1m to 1.4m, 2 – x from 1.4m to 1.8m

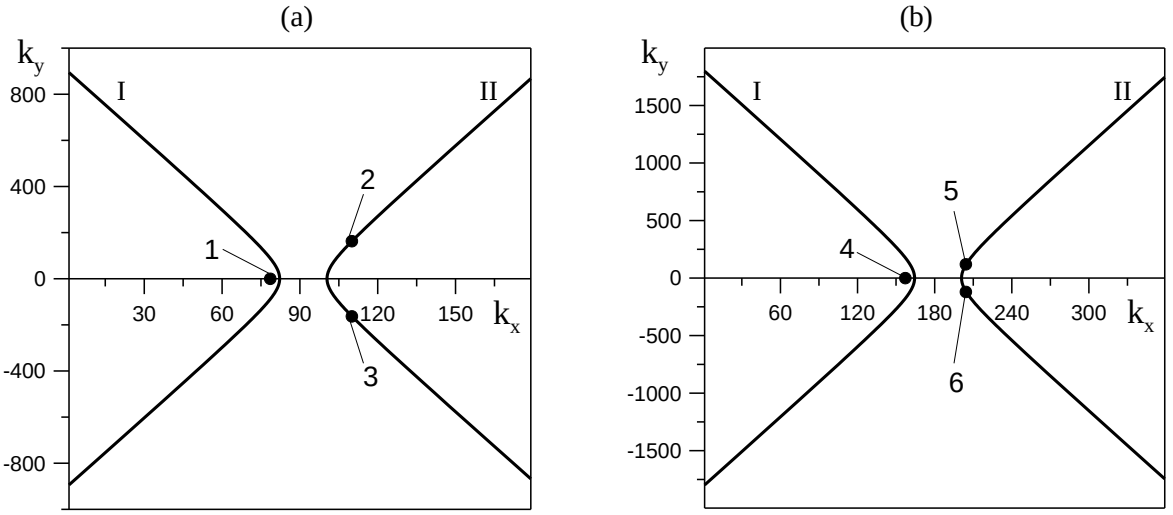

Figure 8. Wave diagrams for acoustic disturbances for f = 40 kHz –(a) and f = 80 kHz – (b): I – fast acoustic waves, II – slow, 1-6 – numerical wave numbers of disturbances in the nozzle channel

The region 1 corresponds to x from 1m to 1.4m, the region 2 corresponds x from 1.4m to 1.8m (the output of the nozzle channel). Figure 8 shows the wave diagrams for acoustic disturbances produced in accordance with the dispersion relations [5] for the frequency f_0=40 kHz (figure 8a) and f_1=80 kHz (figure 8b). Figure 7 shows that there is only one peak at the region 1 (line 1), and there are two peaks of amplitude at the region 2 (line 2). Figure 8 shows that the first peak corresponds to the fast acoustic wave propagating along the nozzle axis (points 1,4), and the second peak corresponds to the amplitude of slow acoustic wave with propagation angles $\beta = 60°$ for $f_0 = 40$ kHz (points 2,3) and $\beta = 30°$ for $f_1 = 80$ kHz (points 5,6). These slow acoustic waves are probably generated by the turbulent boundary layer on the walls of the nozzle as a result of its interaction with the fast mode perturbation.

6. Conclusion

The numerical and experimental investigations of the mode composition of disturbances in hotshot wind tunnel IT- 302M ITAM SB RAS were performed.

It was found that acoustic disturbances in the prechamber of wind tunnel IT-302M generate perturbations corresponding fast acoustic waves propagating along the nozzle axis. The fast acoustic disturbances propagating downstream lead to the appearance of inclined slow acoustic wave of smaller amplitude.

Acknowledgements

This work was supported by the Russian Foundation for Basic Research (Grant No. 16-08-00674) and by the Grant of the Government of the Russian Federation for Supporting Research Supervised by Leading Scientists (Agreement No. 14Z50.31.0019).

References

[1] Maslov A A, Mironov S G, Kudryavtsev A N, Poplavskaya T V and Tsyryulnikov I S 2010 *J. Fluid Mech.* **650** 81–118
[2] Maslov A A, Mironov S G, Poplavskaya T V and Tsyryulnikov I S 2010 *J. Appl. Mech. Tech. Phys.* **51** 482–8
[3] Kirilovskiy S V, Maslov A A, Poplavskaya T V and Tsyryulnikov I S 2015 *Technical Physics Letters* **41** 184–6
[4] Kirilovskiy S V, Maslov A A, Poplavskaya T V and Tsyryulnikov I S 2015 *Technical Physics* **60** 645–55
[5] McKenzie J F and Westphal K O 1968 *Phys. Fluids* **11** 2350–62